*Int. J. Electrochem. Sci.*, 7 **(2012)** 136 - 149

International Journal of
ELECTROCHEMICAL
SCIENCE
www.electrochemsci.org

# Mortars Modified with Geothermal Nanosilica Waste: Effect on the Electrochemical Properties of Embedded Steel Rods

*R. Puente-Ornelas[1,*], L.Y. Gómez-Zamorano[1], M.C. Alonso[2], P.C. Zambrano[1,3], A.M. Guzmán[1], E. Rodríguez[1], B. Bermúdez-Reyes[3], M. Sánchez-Moreno[2]*

[1] Universidad Autónoma de Nuevo León. FIME, Centro de Investigación e Innovación Tecnológica, Av. Universidad s/n. Ciudad Universitaria. San Nicolás de los Garza, Nuevo León, México.
[2] Centro de Investigación en Seguridad de Estructuras y Materiales (CISDEM), CSIC-UPM, C/ Serrano Galvache 4, 28033, Madrid.
[3] Universidad Autónoma de Nuevo León. FIME, Centro de Investigación e Innovación en Ingeniería Aeronáutica. Av. Universidad s/n. Ciudad Universitaria. San Nicolás de los Garza, Nuevo León, México.
[*]E-mail: ropuor@gmail.com

*Received:* 2 November 2011 / *Accepted:* 11 December 2011 / *Published:* 1 January 2012

Nowadays, it is a common practice the incorporation of industrial wastes as alternative materials to replace ordinary Portland cement in the concrete manufacture. This technological implementation has as main objectives, the enhancement of concretes properties as well as mitigation of durability problem related to the corrosion phenomena; in order to increase the service life of reinforced concrete structures. Therefore, in this research was studied the electrochemical properties of black steel embedded in mortars. Mortars were fabricated using as a partial substitute of cement (0, 10, 20 and 30 wt. %) a geothermal nanosilica waste composed of amorphous nanosilica of ~20ηm and chlorides (0 and 0.4 wt. %). Mortars were subjected to a cure at 20°C (80% of relative humidity) and 60ºC (100% of relative humidity). The corrosion behaviour was periodically monitorized up to 65 days using electrochemical techniques of corrosion potential ($E_{corr}$) and corrosion current density ($i_{corr}$). Values of current density ($i_{corr}$) were obtained by linear polarization resistance (LPR) technique applying Stern-Geary relation to $R_p$ values. Electrochemical results were validated by comparing with gravimetric losses. The porosity, pH and loss of the evaporated water were also evaluated in mortars. Results obtained showed that the integrity of reinforcement rods was affected with the increase of GNW at high temperatures as well as the total chlorides content in mortars.

**Keywords:** Reinforced concrete structures, corrosion rate, corrosion potential, linear polarization resistance, geothermal nanosílica waste, Portland cement.

## 1. INTRODUCTION

In the present, there are some environmental problems of enormous importance related with emissions of $CO_2$ by the cement industry around 7% [1-2] and the increase in industrial waste generation.

These two environmental problematic have raised awareness in mankind and aroused their interest in solving them. For this reason, the global trend in industry and construction materials research is oriented to incorporate in the construction process, new materials and/or industrial wastes as substitution materials, partial or total, of Portland cement. This fact not only causes tremendous advantages in the natural resource saving for energy generation and $CO_2$ emissions mitigation, but it contributes to the improvement of mechanical and chemical properties, durability, price and quality of concretes [3-8].

This improvement is attributed to the pozzolanic property that often has many materials, which is utilized to generate hydration reactions with calcium hydroxide (CH) [9-11]. The calcium hydroxide (CH) is a by-product of Portland cement hydration, and it promotes precipitation of calcium silicate hydrated (CSH gel), so that there is a cementing matrix densification and that is reflected by a microstructural uniformity, low porosity and permeability, increased mechanical strength and durability [12].

It is important to mentioned, that many durability problems in existing constructions as expansion, cracking and corrosion of reinforced bars (latter, only in the U.S. causes annual economic losses exceeding $ 300,000 USD billion [13]) were partially offset by the use of materials and/or pozzolanic waste in many studies. Little literature exists for the use of waste generated by geothermal power plants.

These residues cause a number of problems in geothermal power plants due to its high volume generation and accumulation. It is estimated that over 80% of these plants have great difficulty because of the waste.

However, global electrical energy generation through the use of geothermal power is increasing, due to the economic and ecological benefits that represent its use compared with other electrical generation sources [14].

In Mexico, only in the geothermal plant of Cerro Prieto (located in Baja California, North of Mexico), it has been generated more than 70 thousand tons annually [15] of silica-rich wastes called geothermal nanosilica waste (GNW). Therefore, it is of national and international importance its potential application. This residue is a material composed by amorphous silica nanoparticles (~ 20nm) in more than 90 wt. % and considerable amounts of sodium and potassium chlorides [16]. This material has been studied as secondary material in the production of glass, ceramics and refractory [17] as well as in the preparation of pastes [18].

However, there is not reported literature on the study of deterioration caused by corrosion of embedded steel in mortars and concretes modified with geothermal nanosilica waste. Taking into account the above mentioned, in the present research the electrochemical behavior of black steel embedded in mortars modified with GNW was studied.

## 2. EXPERIMENTAL PROCEDURE

### *2.1. Raw materials*

The geothermal nanosilica waste (GNW) provided by the geothermal plant of Cerro Prieto (located in Baja California, North of Mexico) was washed in water at 100°C because it contained high concentrations of sodium and potassium chlorides. This washing was done in order to obtain the desired concentrations of total chloride, 0, 0.4 and 1 wt. % of total chlorides ($Cl^-$) with respect to the cement weight, which were determined via volumetric titration using the Mohr method [19]. After washing, the GNW was dried for 24 h at 120°C in an electrical oven. Subsequently the GNW was sieved to obtain particles below 75 µm and finally homogenized.

The GNW and composite Portland cement (CPC) used in this study were characterized by X-ray fluorescence. In addition, it was determined its density using the Le Chatelier method specified by ASTM C-188-95 standard [20], the surface area using the nitrogen adsorption technique along with the Brunauer Emmett Teller (BET) analysis method. The chemical composition by X-ray fluorescence and physical properties of GNW, as well as, the cement are shown in Table 1.

**Table 1.** Chemical composition (wt. %) of the cementitious materials.

| | CPC | GNW |
|---|---|---|
| $Na_2O$ | 0.36 | 0.32 |
| MgO | 1.27 | - |
| $Al_2O_3$ | 4.46 | 0.09 |
| $SiO_2$ | 18.51 | 98.36 |
| $P_2O_5$ | 0.08 | - |
| $SO_3$ | 3.26 | 0.03 |
| $Cl^-$ | - | 0.06 |
| $K_2O$ | 0.87 | 0.23 |
| CaO | 67.45 | 0.45 |
| $TiO_2$ | 0.21 | - |
| $Mn_2O_3$ | 0.13 | 0.05 |
| $Fe_2O_3$ | 2.61 | 0.04 |
| Loss of ignition | 0.79 | 0.31 |
| Insoluble residues | - | 0.05 |
| Total | 100.00 | 100.00 |
| Pysical properties | | |
| Density ($g/cm^3$) | 3.03 | 2.04 |
| BET area ($m^2/g$) | 0.88 | 8.57 |

Mortars were prepared using 20x50.5x80 mm prismatic molds and reinforced with structural steel using: Type I composite Portland cement (CPC 30R) used according to ASTM C 150-02 Standard [21]; sand standardized, GNW according to ASTM C 618-03 Standard [22], with a total chloride concentrations of 0 and 0.4 wt. % with respect to the weight of cement and distilled water. Used ratios sand/cement and water/cement were 3:1 and 0.5 respectively, and replacement levels of Portland cement by GNW at 0, 10, 20 and 30%. Dosification of raw materials used is shown in Table 2.

**Table 2.** Mix proportions of mortars fabricated.

| | Replacement level of CPC by GNW (%) | | | | | |
|---|---|---|---|---|---|---|
| | 100% | 90%R | 90%R | 90%R | 80%R | 70%R |
| | 0%R | 10%R | 10%R | 10%R | 20%R | 30%R |
| Cement | 22.22 | 20 | 20 | 20 | 17.77 | 15.55 |
| Geothermal nanosilica waste | - | 2.22 | 2.1336 | 2.0031 | 4.44 | 6.66 |
| Sand aggregate | 66.66 | 66.66 | 66.66 | 66.66 | 66.66 | 66.66 |
| Total chlorides (0, 0.4 and 1%) | 0 | 0 | 0.0884 | 0.2189 | 0 | 0 |
| Water | 11.11 | 11.11 | 11.11 | 11.11 | 11.11 | 11.11 |
| Total | 100 | 100 | 100 | 100 | 100 | 100 |

*2.2. Measurement methods*

Structural steels were pickled using a 1:1 solution of hydrochloric acid, washed in acetone and water, and dried with hot air. It was established in the structural steel an exhibition area of 5.67 $cm^2$. Reinforced mortars were subjected to setting and curing conditions: 20°C (80% relative humidity (RH)) and 60°C (100% RH) for 24 hours. They were monitored for 65 days by testing in-situ electrochemical technique using polarization resistance (Rp) [23] with a potentiostat-galvanost (ACM INSRUMENTS GillAC 1199) and a calomel reference standard electrode. Corrosion potential measurements ($E_{corr}$) were taken between the rod and the reference electrode, and values obtained were interpreted according to ASTM C-876-99 [24]. Rp values were processed into corrosion current density ($i_{corr}$) using the Stern and Geary equation [25], considering B = 26 mV. According to $i_{corr}$ values, it was possible to estimate the weight loss associated with these electrochemical measurements using Faraday's law. The interpretation of the $i_{corr}$ values was performed according to the classification proposed by the interamerican network DURAR [26]. Considering $E_{corr}$ and $i_{corr}$ results, mortars which its rods showed signs of corrosion were selected. Rods of these mortars were evaluated by: average $E_{corr}$ and $i_{corr}$, electrochemical loss (EL) from the values of $i_{corr}$ and by the difference in weight (etching the rods at the end of test), gravimetric loss (GL). For mortars, it was evaluated evaporable water loss (% EWL), porosity (% P) and pH.

## 3. RESULTS AND DISCUSSION

Figures 1 and 2 show corrosion potential results ($E_{corr}$) of embedded steels in mortars that were exposed in a setting and curing process at 20°C (80% RH) and 60°C (100% RH) respectively. Horizontal lines indicate limits for the ranges of corrosion probability according to the ASTM C876-99 Standard.

In Figure 1, is observed that the majority of embedded steels in cured mortars at 20°C (with 80% RH) showed a 50 % of corrosion probability (between -250 and -350 mV) during the first 7 days. This phenomenon is attributed that during this first days of curing, the mortar cement matrix was poor in hydrated products generated by cement as the CSH gel and portlandite. The latter, being in low concentration led to the nill generation of CSH gel due to the pozzolanic reaction between it and the GNW.

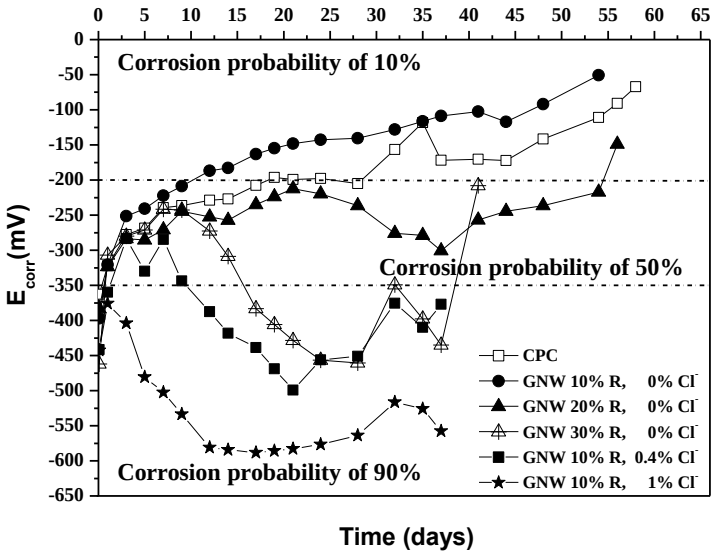


**Figure 1.** The corrosion potential ($E_{corr}$) versus time for steel bars embedded in designed mortars. The specimens were subjected at 20°C, 80%RH.

As a result of this phenomenon, mortars registered a high porosity. Coupled with this, the water instauration in pores (as they are in an atmosphere of 80% RH) lead to a favored inclusion of oxygen through the cement matrix and pores. That was the main reason why embedded steels in mortars presented the corrosion probability values cited above.

On the other hand, embedded steels in mortars designed with 1% total chlorides showed a high corrosion probability during the first hours of curing. This phenomenon can be also related to the degree of hydration of the cement matrix, which was poor in CSH gel contents. Consequently, the matrix was more porous; therefore the mobility of $Cl^-$ and $O_2$ was favored and a corrosion probability of 90% (-350 and between -650 mV) in these steels was promoted.

In the figure 1, can be observed the behavior exhibited in steels when the mortars reached 14 exposure days. In the case of embedded steels in mortars with addition of 0, 10 and 20 wt. % GNW, corrosion probability of 10% (between -250 and 0 mV) was observed. The corrosion probability of these steels tended to decrease with a curing time increase; this behavior was attributed to a greater

CSH gel presence in the cement matrix in comparison with the contents exhibited within the first 7 days of curing.

In these mortars, the cement grains were partially or completely reacted, and after that, there was also an increased release of portlandite which was used by the GNW to react with and produce more CSH gel, which also promoted in the mortar a more densified cement matrix.

This decrease in corrosion probability was not observed in embedded steels corresponding to mortars with 30 wt. % GNW addition. This behavior can be attributed to a greater porosity degree in comparison with mortars containing 10 and 20 wt. % GNW. It is suggested that porosity was developed during the mixing process since the workability was not good in comparison with that of mortars with addition of 10 and 20 wt. % GNW.

Since GNW surface area is very large, it demanded a large water amount that was not added during the mixing process, which produced GNW agglomerates. This condition affected significantly the workability of the mixture; thus the result was the presence of large porosity. However, it can be seen that despite this, the corrosion probability in these steels in the last days of monitoring tended to decrease, which was due to the cement matrix is continuously in densifying thanks to the production of CSH gel as reaction product of anhydrous cements and GNW with CH. Moreover, for the case of embedded steels in mortars designed with 0.4 and 1% of total chlorides, figure 1 showed an increase in the corrosion probability with time from 14 days of curing, which is attributed to the presence of chloride ions in the pore solution.

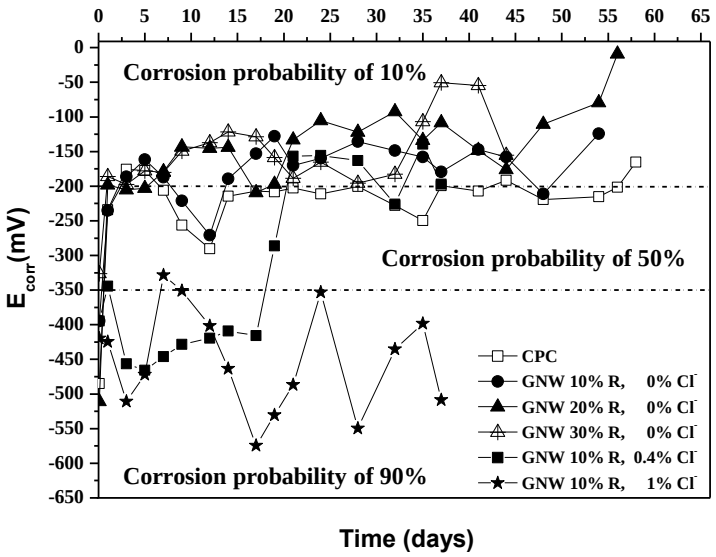


**Figure 2.** The corrosion potential ($E_{corr}$) versus time for steel bars embedded in designed mortars. The specimens were subjected at 60°C, 100% RH.

Figure 2 shows electrochemical results obtained in embedded steels in mortars cured at 60°C (100% RH). Through these results, it can be seen that all embedded steels in mortars whose mixing design contains 0% of total $Cl^-$ had a corrosion probability of 10% (between -250 and 0 mV) in the first hours of curing, which practically remained at these values until the end of the electrochemical tests. This behavior was attributed to hydration reactions of cement materials at elevated temperatures

[27, 28]. In this particular case, these reactions were made very quickly, especially before the first 7 curing days; so that, the hydrated products of cement in comparison with those typically exhibited at low temperatures (10 - 30°C) are higher. For that reason, the cement matrix was slightly denser and lesser permeable at 60°C than at 20°C.

However, it was observed that the electrochemical tendency of steels was hardly changed over time, showing a slight shift of corrosion potential values in the direction of 0 mV with respect to values presented before the 7 curing days. This was mainly because a little contribution of CSH, that even in small amounts leads to densifying the cement matrix of the mortars, making it less porous over time. This low contribution of CSH gel at 60°C is due to at this condition, this hydrated product of cement is usually generated in a heterogeneous distribution within the cement matrix. Since at this temperature there is insufficient time for distribution and arrangement of hydrated products, these products tend to settle on the anhydrous cement grains forming a dense layer, which enables a delay in the subsequent hydration rate of partially reacted cement grains [29]. For this reason, it is generated little amount of CSH gel over time and it is reflected in electrochemical results obtained in steels at this current condition.

According to the electrochemical behavior exhibited by embedded steels in mortars designed with 0.4 and 1% of total chlorides, it was observed that these steels present a corrosion probability of 90% at early stages of the curing process. It can be attributed to a greater solubility and mobility of chloride ions in the cement matrix at 60°C, so there is a possibility to promote this corrosion probability exhibited by steels.

Figures 3 and 4 show corrosion rate results ($i_{corr}$) of embedded steels in mortars that were exposed in a setting and curing process at 20°C (80% RH) and 60°C (100% RH). Horizontal lines indicate limits for the ranges of corrosion probability according to interamerican network DURAR. Note that the dotted horizontal line in the $i_{corr}$ value of 0.2 $\mu A/cm^2$ indicates, according to some researchers, that the steel corrosion may be occurring in the range of 0.1-0.2 $\mu A/cm^2$ [30].

Figure 3 shows that the majority of embedded steels in cured mortars at 20°C (80% RH) exhibited during the first days of the setting and curing process, moderate and low corrosion levels (between 0.1 and 1 $\mu A/cm^2$). After 5 days of curing, it can be seen that embedded steels in mortars with substitution of CPC by GNW (10, 20 and 30 wt. % R) had a negligible corrosion level (between 0.03 and 0.07 $\mu A/cm^2$). This corrosion level showed a tendency over time to reach lower corrosion current density values, which can be explained in terms of time; since as time passage, it generates a denser cement matrix which reduces the porosity of mortars; consequently, the passivity of embedded steels is favored.

Regarding embedded steels in mortars with 0.4 wt. % of total chlorides content, it showed that the amount of chloride contained in the cement matrix slightly favored the corrosion over time but it was negligible (between 0.04 and 0.07 $\mu A/cm^2$). However, this type of corrosion had a slight tendency to destabilize the passive film formed on steels, since current density values were closer to 0.1 $\mu A/cm^2$. This fact can result that steels reach, in certain times, low corrosion levels at older ages.

In addition, it can be seen that embedded steels in mortars with contents of 1% of total chlorides, presented during the first days of curing a moderate corrosion level (between 0.5 and 1 $\mu A/cm^2$). After 7 curing days, a low corrosion level (between 0.1 and 0.2 $\mu A/cm^2$) was observed.

According to the tendency of obtained values, it is possible that over time these steels can present a pitting corrosion. The activation mechanism of this type of corrosion can be due to chlorides. Once hydrated phases get saturated on the cement matrix (CSH gel), these are deposited in the pore solution, so they are available to generate this localized corrosion phenomenon in steels.

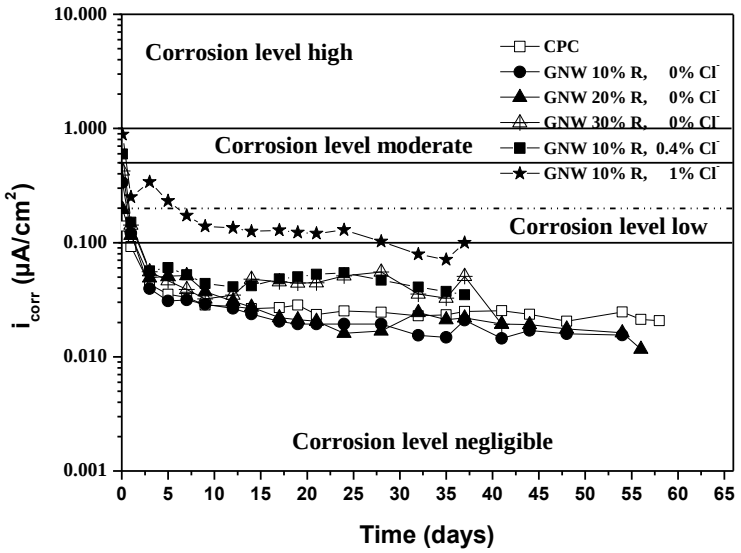


**Figure 3.** Corrosion rate ($i_{corr}$) versus time for steel bars embedded in the different mortars. Specimens were subjected at 20°C, 80% RH.

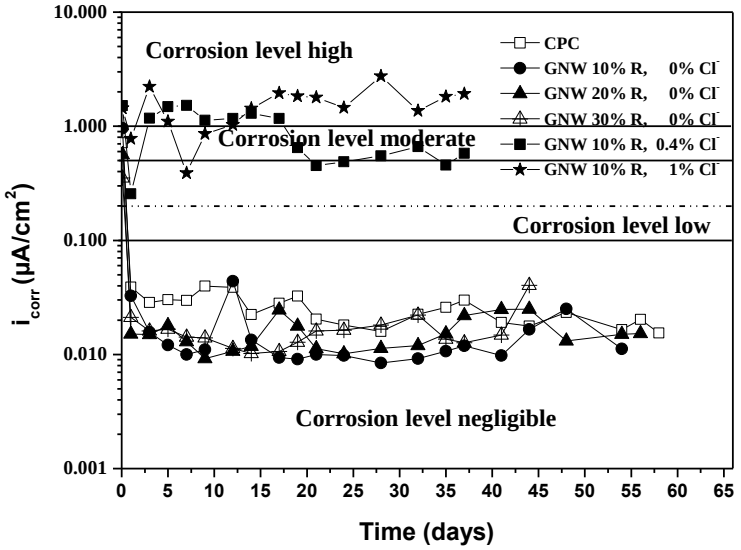


**Figure 4.** Corrosion potential ($i_{corr}$) versus time for steel bars embedded in the different mortars. Specimens were subjected at 60°C, 100% RH.

Figure 4 shows that embedded steels in mortars with GNW additions (0, 10, 20 and 30 wt. % R) and cured at 60°C (100% RH) exhibited during the first days of curing a negligible corrosion levels (lesser than 0.05 $\mu A/cm^2$) and over time show a tendency to remain in the same corrosion state.

In the case of embedded steels in mortars with additions of 0.4 and 1% of total chloride, corrosion levels ranging from moderate to high (0.5 to 2 $\mu A/cm^2$) were presented. The high corrosion level is accentuated in early curing days for mortars with 1% of total chlorides.

Moreover, it can be seen that tendency of the corrosion current density values in steels remained constant over time (ie. it is remained at same corrosion levels), even it can overcome these critical values, since pitting corrosion in these special curing conditions may be aggravated over time.

In Figure 5, average values of corrosion potential ($E_{corr}$) and corrosion rate ($i_{corr}$) are presented, which were obtained from results shown and discussed previously. According to the addition effect of GNW on the corrosion rate, it can be seen in Figure 5A that mortars exposed to the environment of 20ºC (80% RH) had relatively higher corrosion rate values compared with those to the environment of 60°C (100% RH) at all substitution levels of GNW with 0 % totals $Cl^-$. This behavior was attributed to the pores network in the mortar, since in 80% RH, this network was partially saturated with water, which leads a greater diffusion of $O_2$ through pores into the cemented matrix in comparison with mortars exposed to 100% RH.

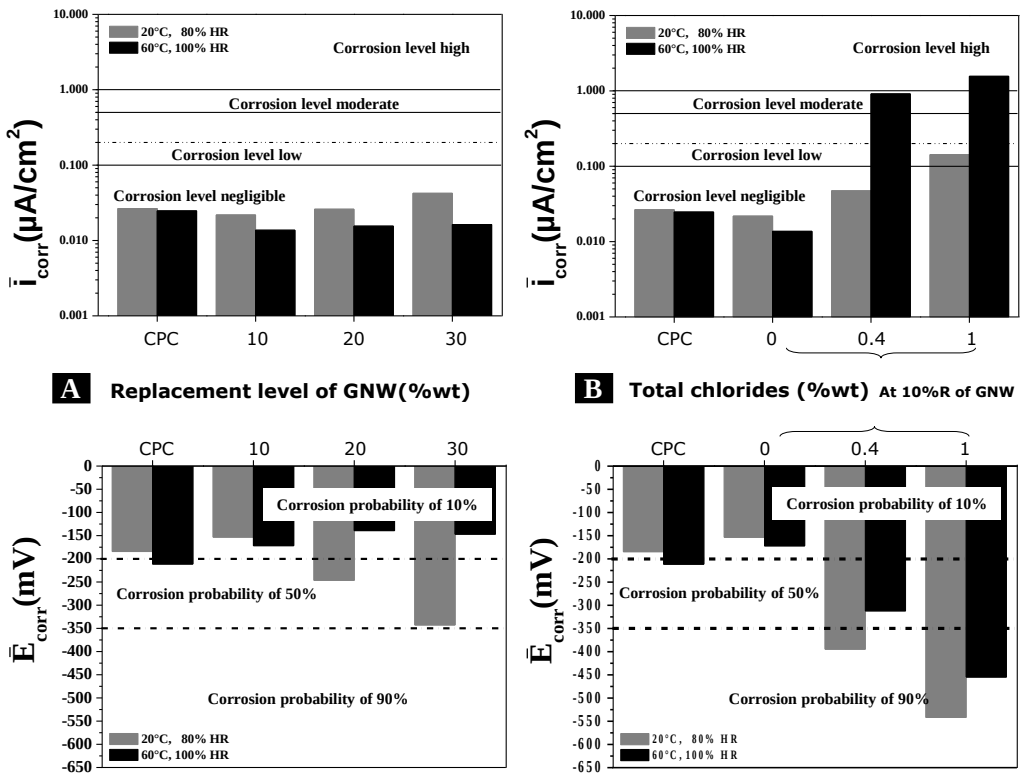


**Figure 5.** Comparison between average values of corrosion potential ($E_{corr}$) and corrosion rate ($i_{corr}$) for embedded steel in mortars made of different mortars and exposed to 20°C and 60°C with 80 and 100% relative humidity respectively : A) Effect of replacement level B) Effect of total chlorides.

On the other hand, embedded steels in mortars with chlorides additions and exposed in the environment of 60ºC, 100% RH, (Figure 5B) registered corrosion rates values that are twice compared to the values obtained in embedded steels at 20°C (80% RH). This was attributed to the constant cycles

of wetting-drying exposed at 60°C and to the high solubility that $Cl^-$ ions presented in this condition [31-33]. This condition leads to precipitate these ions in the pore solution, which was saturated with water and thus $Cl^-$ ions were available to cause a high degree of corrosion on reinforcement steel. This was evidenced by extracting the embedded steel from mortars with 10% added GNW and 0.4% total chlorides, these steels showed the highest degree of pitting corrosion in the exhibition area as illustrated in figure 6.

This phenomenon was not observed at 20°C, $Cl^-$ ions in this condition were absorbed by certain components present in the cement matrix, such as CSH gel, but mainly by the aluminate phase and in the latter unleashed the formation of Friedel salt [34, 35]. So that, there were few $Cl^-$ ions available in the pore solution to generate pitting corrosion, that is why the risk of corrosion of steels exposed in the condition of 20°C became lesser susceptible than in the case of those exposed in the condition of 60°C.

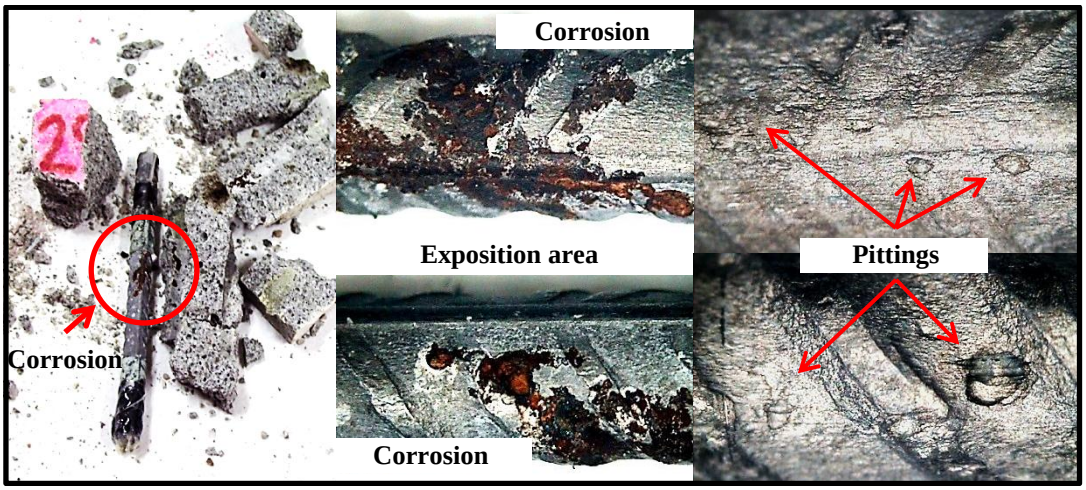


**Figure 6.** Passivity state exhibited in embedded steels in mortars with 10 wt. % of GNW with 0.4 wt. % of total $Cl^-$ (cured at 60°C and 100% RH).

These electrochemical results shown by steels can be explained based on the determination of the physical properties of mortars in which they were embedded, whose results are shown in Table 3. In this regard, it was observed that mortars exposed to the atmosphere of 100% RH showed a higher percentage of evaporable water loss (% E.W.L) than those exposed to 80% RH. This effectively means that in the condition of 100 % RH there was more water in the pore solution comparing to the 80% RH condition, which prevented the passage of $O_2$ to the reinforcement steel, therefore, these steels had less risk of corrosion in the condition of 100% RH with respect to 80% RH.

Regarding the results of electrochemical losses (E.L.) and gravimetric losses (G.L), most of them were shown to have good correlation between both techniques, which means that the linear polarization resistance technique (Rp) was used in an adequate manner and proved to be reliable for electrochemical measurements at laboratory level.

In the case of results exhibited by embedded steels in mortars with 10 wt. % of GNW addition without $Cl^-$ contents and cured at 60°C do not show good correlation. This was attributed to the

corrosion presence under the tape in some steels after being extracted from the mortar; since after removing the tape, it was detected rust between the exposed area and the tape. This oxidation caused an increase in material losses (in steels), whose values were detected by the electrochemical technique. However, when electrochemical calculations were performed, the corrosion under tape was not considered. Therefore, a not good correlation was found between the electrochemical and gravimetric results in these steels.

In accordance to results of total porosity tests (% P), it can be seen that the % P was increased with increments in GNW, chlorides contents and curing temperature. The above mentioned was attributed to the GNW particle size (~ 20 ηm), which demands during the mortar mixing process, a large water amount to cover GNW particles in order to achieve reactions conditions. So the workability of mixtures was affected and consequently promoted the formation of GNW agglomerates causing a decrease in mixture homogeneity. In the same way, it happens with chlorides. Once they get hydrated much large water content was needed and this fact also contributes to the decrease in mixture workability. In both cases, the workability was affected; it is due to an increase in porosity of the mortars caused by the GNW and chlorides additions.

The difference in results taking into account the porosity percentage with respect to the temperature increase was mainly attributed to the rate increase in the hydration reactions of cement materials carried out at 60°C. It promoted the formation of a dense layer of hydrated products around the partially reacted cement grains, so that the rate in subsequent hydration reactions of these grains decreases dramatically, impacting with a drop of CSH gel production.

**Table 3.** Characterization results of mortars and steels after electrochemical testing.

| | Replacement level of CPC by GNW and curing environment | | | | | | |
|---|---|---|---|---|---|---|---|
| | 10%R 0%$Cl^-$ | 30%R 0%$Cl^-$ | 10%R 0.4%$Cl^-$ | 10%R 1%$Cl^-$ | 10%R 0%$Cl^-$ | 10%R 0.4%$Cl^-$ | 10%R 1%$Cl^-$ |
| Properties | 20°C 80%RH | 20°C 80%RH | 20°C 80%RH | 20°C 80%RH | 60°C 100%RH | 60°C 100%RH | 60°C 100%RH |
| G.L | 0.00088 | 0.00142 | 0.00158 | 0.00119 | 0.00232 | 0.00584 | 0.00809 |
| E.L. | 0.00037 | 0.00057 | 0.00061 | 0.00154 | 0.00034 | 0.00879 | 0.01695 |
| %E.W.L | 7.22 | 7.81 | 7.07 | 7.4 | 8.44 | 8.05 | 8.49 |
| %P | 16.62 | 18.2 | 18 | 18.27 | 23.63 | 24.17 | 24.29 |
| pH | 12.74 | 12.61 | 12.73 | 12.63 | 12.68 | 12.67 | 12.59 |
| *$E_{corr}$ | -153.22 | -342.76 | -394.6 | -541.64 | -171.63 | -311.79 | -454.59 |
| *$i_{corr}$ | 0.022 | 0.042 | 0.047 | 0.14 | 0.014 | 0.913 | 1.56 |

*Note: The potential corrosion ($E_{corr}$) and corrosion rate ( $i_{corr}$) are given as average values.

This latter behavior caused the formation of a heterogeneous cement matrix composed by hydrated products, thus over time it will reflect high porosity in mortars. This behavior did not happen

at 20°C because at this curing temperature, hydration reactions of cement materials were taken place in a slow manner. Therefore, it was facilitated the formation of CSH gel and CH, due to that it was achieved a more compact cement matrix with less porosity in the analyzed mortars.

Regarding the results obtained, concerning the pH tests conducted in mortars, it can be observed that values tend to decrease as GNW addition is increased. It was attributed to consumption of portlandite by the GNW. These two compounds react and produce CSH during the hydration process, thus causing a decrease in pH. A phenomenon also observed with the addition of chlorides in mortar mixtures, as they reacted with hydrated aluminate phase to form Friedel's salt, which also consumed portlandite during its formation, thus causing a decrease in the alkalinity of the mortars [36, 37].

## 3. CONCLUSIONS

Electrochemical results showed that it is possible to use geothermal nanosilica waste as replace materials ranging from 0% of total chlorides up to 30 wt. % without affects reinforced steels by corrosion phenomena.

Embedded steel used in mortar with 10 and 20 wt. % of geothermal nanosilica waste showed lesser corrosion probability values comparing to those exhibited by embedded steels in mortars made with 100 wt. % of CPC.

Particularly, mortars replaced with 10 wt. % of geothermal nanosilica waste and cured at 20°C (80% RH) and 60°C (100% RH) were found to have better properties against corrosion, since values of $i_{corr}$ and $E_{corr}$ represent less corrosion probability compared with those exhibited by a mortar made with 100 wt. % of CPC.

It is possible to incorporate in the mortar mixture design a 10 wt. % geothermal nanosilica waste with contents of chloride up to 0.4 wt. % with respect to the amount of cement material, without affecting embedded steels in mortars by pitting corrosion phenomena as long as mortars are subject to a 20°C work environment.

The curing temperature, coupled with the presence of chloride, significantly affects hydration processes, so that at high temperatures presents aggressive phenomena such as pitting corrosion, reducing the durability of mortars.

## References

1. E. M. R. Fairbairn, B. B. Americano, G. C. Cordeiro, T. P. Paula, R. D. Toledo Filho, M. M. Silvoso, *J. Environ. Manage.* 91 (2010) 1864 – 1871.
2. E. Worrell, L. Bernstein, J. Roy, L. Price, J. Harnisch, *Energy Efficiency*, 2 (2009) 109-123.
3. S. Harsh, A. K. Arora, M. M. Ali, M. Vasudeva, Proceedings of XIII ICCC International Congress on the Chemistry of Cement, Madrid, Spain, (2011).
4. M. Nehdi, J. Duquette, A. E. Damatty, *Cement Concrete Res.*, 33 (2003) 1203-1210.
5. E. P. Reyes-Diaz, E. B. Maldonado, F. Almeraya, D.M. Bastidas, M.Z. Baltazar, J. Chacón, A. Martínez-Villafañe, J.M. Bastidas, C. Gaona-Tiburcio, *Int. J. Electrochem. Sci*, 6 (2011) 1892-1905.

6. E. E. Maldonado-Bandala, V. Jiménez-Quero, F. J. Olguin-Coca, L. G. Lizarraga, M. A. Baltazar-Zamora, A. Ortiz, F. Almeraya, P. Zambrano, C. Gaona-Tiburcio, *Int. J. Electrochem. Sci.*, 6 (2011) 4915 – 4926.
7. S. P. B. Lima, G. C. Cordeiro, A. O. Paiva, M. R. M. Chaves, R. P. Vasconcelos, F. R. D. Toledo, E. M. R. Fairbairn, Proceedings of XIII ICCC International Congress on the Chemistry of Cement, Madrid, Spain, (2011).
8. V. M. Malhotra, Proceedings of International Symposium on Durability of Concrete, Monterrey, México, (2005).
9. A. Korpa, T. Kowald, R. Trettin, *Cement Concrete Res.*, 38 (2008) 955–962.
10. L. Muhmood, S. Vitta, D. Venkateswaran, *Cement Concrete Res.*, 39 (2009) 102–109.
11. E. Güneyisi, M. Gesoglu, *Mater. Struct.*, 41 (2008) 479–493.
12. A. Cwirzen, V. Penttala, C. Vornanen, *Cement Concrete Res.*, 38 (2008) 1217–1226.
13. M. J. Lieser, C. Stek, *OCV, Reinforcements*, November (2010).
14. Comisión Federal de Electricidad, http://www.cfe.gob.mx.
15. A. Camenzuli, G. M. Mudd, 3rd International Conference on Sustainability Engineering & Science: Blueprints for Sustainable Infrastructure Auckland, New Zealand, (2008).
16. L. Y. Gómez, J. I. Escalante, G. Mendoza, *J. of Materials Science Letters*, 39 (2004) 4021-4025.
17. J. Rincon, M. Romero, C. Díaz, V. Balek, Z. Malek, *J. Therm. Anal. Calorim.*, 56 (1999) 1261-1269.
18. L. Y. Gómez, J. I. Escalante, 12th International Congress on the Chemistry of Cement, Canada, (2007).
19. D. Skoog, D. West, F. Holler, Química Analítica, 6 Ed. Mc Graw-Hill, México, (1995).
20. ASTM Standard C 188-95, Test Method for Density of Hydraulic Cement West Conshohocken, PA, American Society for Testing and Materials, (1995).
21. ASTM C 150-02 Standard Specification for Portland cement test, West Conshohocken, PA, American Society for Testing and Materials, (2002).
22. ASTM C 618-03 Standard Specification for fly ash and raw coal or natural calcined puzzolo for use as a mineral admixture in concrete, West Conshohocken, PA, American Society for Testing and Materials, (2003).
23. S. Feliú, J. A. González, C. Andrade, "Electrochemical Methods for On-Site Determinations of Corrosion Rates of Rebars". Techniques to Assess the Corrosion Activity of Steel Reinforced Concrete Structures. ASTM STP 1276. Neal S. Berque, Eduard Escalante, Charles K. Nmai and David Whiting, Eds., American Society for Testing and Materiales, (1996).
24. ASTM Standard C 876-99, Test method for half-cell potentials of uncoated Reinforcing Steel in Concrete. West Conshohocken, PA, American Society for Testing and Materials, (1999).
25. M. Stern, A. L. Geary, Journal of the Electrochemical Society, 104 (1957) 56.
26. DURAR NETWORK, Manual Inspection Evaluation and Assessment of Corrosion in Reinforced Concrete Structures, CYTED Program, Rio de Janeiro (1997).
27. J. I. Escalante-Garcia, J. H. Sharp, *Cement Concrete Res.*, 31 (2001) 695–702.
28. K. Ezziane, A. Bougara, A. Kadri, H. Khelafi, E. Kadri, *Cement Concrete Comp.*, 29 (2007) 587–593.
29. M. M. Canut, M. R. Geiker, Proceedings of XIII ICCC International Congress on the Chemistry of Cement, Madrid, Spain, (2011).
30. C. Andrade, C. Alonso, *Constr.Build. Mater.*, 10 (1996) 315-328.
31. C. Andrade, C. Alonso, J. Sarría, *Cement Concrete Comp.*, 24 (2002) 55-64.
32. A. Castillo: "XVI curso de estudios mayores de la Construcción", CEMCO, (2004).
33. C. Andrade, C. Alonso and J. Sarria, *Mater. Construcc.*, 48 (1999) 1-17.
34. American Concrete Institute: "Guía para la Durabilidad del Hormigón", Informado por el Comité ACI 201-2R92, (2000).
35. M. A. San Juan, *J. Mater. Sci.*, 32 (1997) 6207-6213.

36. H. Zibara, R. D. Hooton, M. D. A. Thomas, K. Stanish, *Cement Concrete Res.*, 38 (2008) 422–426.
37. L. Y. Gómez-Zamorano, J. I. Escalante, *Mater. Construcc.*, 59 (2009) 5-16.